journal

J. Am. Ceram. Soc., ■■ [■■] 1–4 (2008)
DOI: 10.1111/j.1551-2916.2008.02488.x

In Situ Monitoring of Structural Changes in Boron Carbide Under Electric Fields

Giovanni Fanchini, Varun Gupta,† Adrian B. Mann, and Manish Chhowalla

Materials Science and Engineering, Rutgers University, Piscataway, New Jersey 08854

***In situ* monitoring of the transformation of B_4C under electric field using Raman spectroscopy is reported. Application of electric fields up to 5000 V/cm leads to local segregation of carbon, indicated by the appearance of Raman D and G peaks. At low electric fields (<3000 V/cm) the segregated carbon is amorphous, while at higher fields aromatic sp^2 clustering is observed. Electrical measurements as a function of temperature are used to complement the Raman measurements. The results demonstrate that it is possible to induce transformations in boron carbide using electric fields that are comparable with those obtained under shock and nanoindentation.**

I. Introduction

The high hardness (~30 GPa) and Hugniot elastic limit (HEL ~17–20 GPa), along with low density, of hot-pressed boron carbide (nominally B_4C)[1] make it an ideal material for ballistic armor applications. In addition, boron carbide possesses the highest dynamic elasticity of ceramic materials.[2] Although these properties would suggest that boron carbide could withstand high-velocity impacts, this has not been observed. The absence of residual plastic strength above the HEL, a compulsory requirement for armor survival upon damage, is thought to be the primary reason for failure of boron carbide at lower than expected impact rates and pressures. This behavior is unique in dynamically elastic materials finding counterparts only at much lower stress values (<1 GPa) in dynamically inelastic ionic insulators, such as quartz and glasses.[3,4] TEM investigation by Chen *et al.* revealed 2–3 nm shock-induced amorphization bands along the (113) crystallographic plane in impact-tested boron carbide.[5] However, no explanation for the origin of these amorphous bands was offered in that report.[5] Our theoretical study revealed that the failure of B_4C is commensurate with the segregation of boron icosahedra embedded in amorphous carbon in 2–3-nm-wide amorphous bands along the (113) crystallographic plane.[6]

In impact studies,[5] postmortem analysis of failed material is usually conducted. Alternatively, Domnich *et al.*[7] utilized *ex situ* Raman measurements to characterize local amorphization induced by nanoindentation. Ge *et al.*[8] demonstrated similar effects in scratch debris on boron carbide. It was also shown in Ge *et al.*[8] that annealing of the scratch debris led to D and G features that were similar to sp^2-rich amorphous carbon (a-C), suggesting clustering. Recent work has suggested that these clusters may also contain boron (i.e., the material is actually a-C:B).[9] In addition, Ge *et al.*[8] detected π-bonded electrons by electron-energy loss spectroscopy, an indication of the presence of sp^2 bonding. In addition to the D and G features, a number of papers[7–10] also reveal a Raman feature at ~1800–1850 cm^{-1} under pressure or after indentation. The peak has been identified at 1810 cm^{-1} by Domnich *et al.*[7] when using 514.5 nm Raman excitation.

Recently, La Salvia *et al.*[11] demonstrated that impacted boron carbide samples exhibited peaks at 1330, 1580, and ~1750 cm^{-1} using a 785 nm Raman laser. The position of the high-frequency peak on impacted samples was lower than that in indented samples (i.e., >1800 cm^{-1}). However, the discrepancy can be explained by the fact that La Salvia *et al.* used an infrared (785 nm) laser for the Raman measurements, while the indent-induced peak at ~1800 cm^{-1} has been generally observed at shorter (i.e., visible light) excitation wavelengths. In fact, Raman measurements on microindented samples recently performed by our group[12] show that the indent-induced feature observed at ~1810–1830 cm^{-1} at blue–green excitation is dispersive and strongly downshifts (to 1700 cm^{-1}) at longer excitation wavelengths.

Real-time Raman characterization could provide valuable insight into why B_4C fails prematurely in dynamic tests. In this work, we show that amorphization in B_4C occurs by the application of relatively low electric fields. By applying pulses of increasing voltage and simultaneously monitoring changes with Raman spectroscopy (Fig. 1(A)), it is possible to observe not only the onset but also the degree of sp^2 clustering in real time. Furthermore, through electrical measurements as a function of temperature in conjunction with Raman spectroscopy, we are able to determine that above a critical electrical field, amorphization leads to partial collapse of the B_4C structure.

II. Experimental Procedure

Highly polished hot-pressed boron carbide with a density close to 100% provided by an industrial supplier was used in this study. The samples were obtained by cross-sectioning a 1-mm-thick central section of a 2.5 cm × 2.5 cm hot-pressed tile. The sample surface was further polished until graphite from the surface was eliminated. There was no significant difference in the Raman spectra obtained from the starting powder (B_4C stoichiometry) and the samples. In addition, there was no contribution to the Raman spectra from the additives used during hot pressing.

The electrical Raman measurements were performed on a Renishaw InVia Raman spectrometer at an excitation wavelength of 785 nm. Gold electrodes (width 1 mm, channel lengths 20 μm) were defined on each substrate using a shadow mask. External voltage pulses of 0–10 V (leading to electric fields, E_{ext}, of 0–5000 V/cm) were applied for 120 s to the electrodes during the Raman measurements using a GW GPS-1850D stabilized power supply. Each series of Raman spectra at varying voltage was recorded on the same spot in order to obtain comparable signal intensities. To eliminate the possibility of Raman laser-induced transformation, we performed similar measurements in the absence of an electric field, which did not show a variation of the spectra with time. The results discussed here are representative of what is observed on a large number of B_4C samples.

G. Subhash—contributing editor

Manuscript No. 24175. Received January 2, 2008; approved April 10, 2008.
This work is funded by NSF DMR (CER) 0604314, NSF IUCRC Ceramic and Composite Material, and US ARL Materials Center of Excellence in Lightweight Materials at Rutgers.
†Author to whom correspondence should be addressed. e-mail: guptav@eden.rutgers.edu

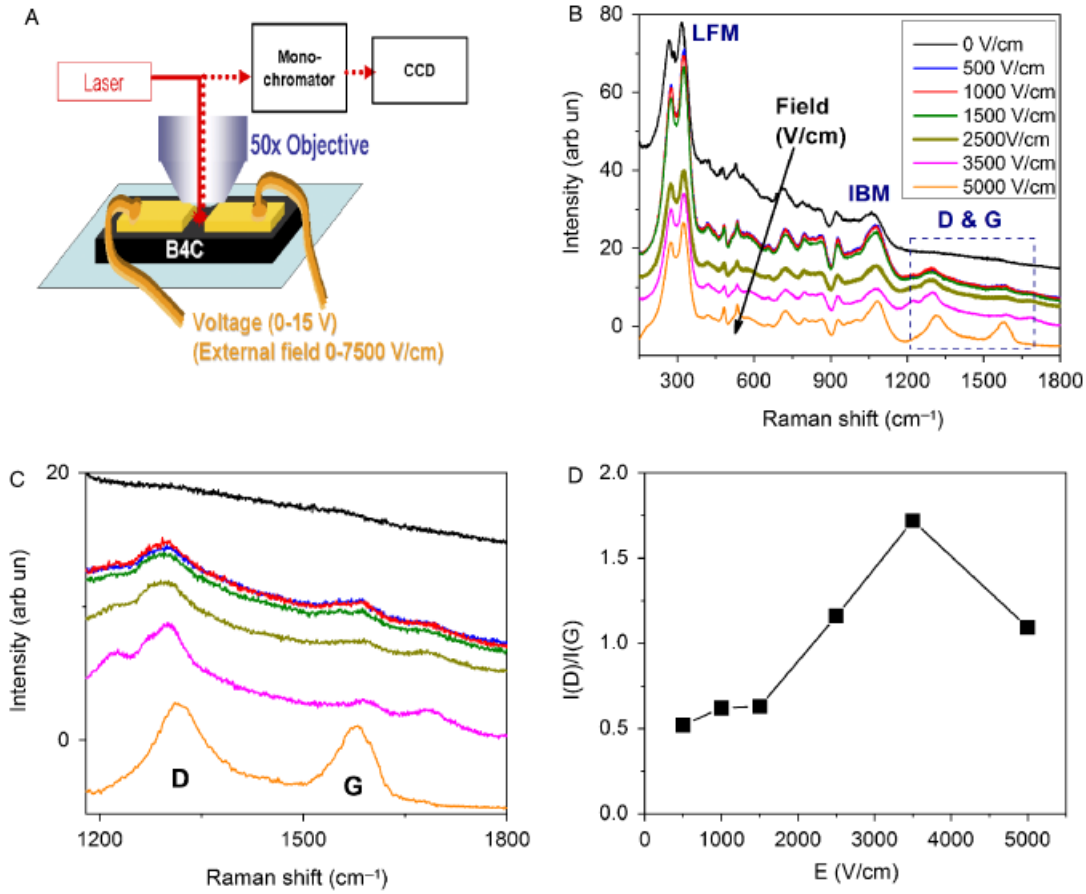

Fig. 1. (A) Schematic of the apparatus used for *in situ* Raman investigation of boron carbide under electric field. Raman spectra as a function of the electrical field showing the (B) entire frequency range, including the boron carbide modes, and (C) detailed plot of the frequency region where the carbon D and G peaks are present and (D) the ratio of $I(D)/I(G)$ vs applied electric field.

III. Results and Discussion

The Raman spectra of hot-pressed B_4C, recorded *in situ* during application of increasing electric field pulses, are shown in Figs. 1(B) and (C). Two primary effects on the Raman spectra with increasing electric fields are evident. First, the decrease in the intensity of the B_4C-related Raman modes (frequencies ranging from 275 cm^{-1} to 1100 cm^{-1}[13,14]) can be seen. Second, the strong increase of the D ($\sim$1300 cm^{-1}) and G ($\sim$1600 cm^{-1}) carbon modes under voltage pulses can be observed in Fig. 1(C). It is also clear in Fig. 1(C) that very weak carbon D and G modes are present in the sample even before electric field is applied. We attribute this to the precipitation of carbon in grain boundaries during densification or to the presence of disordered carbon in as-synthesized powder, as recently reported.[15]

In Fig. 1(C), the Raman modes in the 1200–1700 cm^{-1} range strongly increase in intensity with electric field strength, especially between 1500 and 3500 V/cm where the intensity of the B_4C modes (Fig. 1(B)) was observed to decrease. Furthermore, the broad line widths of the peaks indicate the presence of disordered or amorphous carbon domains rather than ordered graphite.[16] If we tentatively assign the two features at $\sim$1350 and 1580 cm^{-1} to the D and G peaks related to sp^2 clusters of a-C(:B), then the data in Fig. 1(C) reveal that the D peak increases faster in area and intensity than the G peak, leading to an increase in the D/G ratio. Because the D/G intensity ratios in amorphous carbon are proportional to the size, L, of the sp^2 cluster domains through the relationship $I(D)/I(G) \sim L^2$,[16] it can be inferred that the island sizes increase with electric field. As these clusters are aromatic, a similar model valid for amorphous carbon nitride[17] should also apply to boron-containing a-C as we have observed in a separate study.[12] In addition, Fig. 1(D) shows the ratio of $I(D)/I(G)$ vs applied electric field. The D peak arises from aromatic rings so that, for a fixed wavelength, $I(D)/I(G)$ should increase with increasing disorder.[16]

In addition to the D and G modes, supplementary peaks at approximately 1250 and 1700 cm^{-1} are also present in Fig. 1(C). Yan *et al.*,[10] using a shorter Raman excitation wavelength ($\lambda = 514.5$ nm), observed a similar feature at higher frequency (>1800 cm^{-1}). Also, a feature at similar position was detected by Ghosh *et al.*,[9] who suggested that it may be related to a mixed amorphous carbon–boron phase. Using infrared excitation wavelength, La Salvia *et al.*[11] noticed a peak at $\sim$1750 cm^{-1} after the failure of B_4C under ballistic impact. No G peak or other peaks at 1580–1600 cm^{-1} were present, although a peak at $\sim$1300–1350 cm^{-1} (i.e., close in frequency to the carbon D peak) was detected.[11] We will further clarify the origin of this peak in future work.[12] However, the detection of the high-frequency feature between 1700 and 1850 cm^{-1} may suggest that failure by nanoindentation, ballistic impact, and electric field pulses are due to related mechanisms.

At the maximum applied electric field (5000 V/cm), narrow D and G bands indicative of highly sp^2-rich amorphous carbon with relatively large aromatic clusters appear.[16] The presence of the G and D peaks and the disappearance of the subsidiary bands at 1250 and 1700 cm^{-1} indicate that aromatic amorphous carbon clusters are present. Indeed, the spectra at 5000 V/cm resemble those obtained by Ge *et al.*[8] after annealing the scratch debris from boron carbide single crystals. We therefore conclude that application of sufficiently large electric fields leads to carbon segregation and onset of aromatic sp^2 clustering in boron carbide.

To further analyze the structural changes in B_4C observed with Raman spectroscopy, electrical measurements at room and higher temperatures were performed by applying 1–10 V pulses across 20 μm Au gap cells using a GW GPS-1850D (Instek,

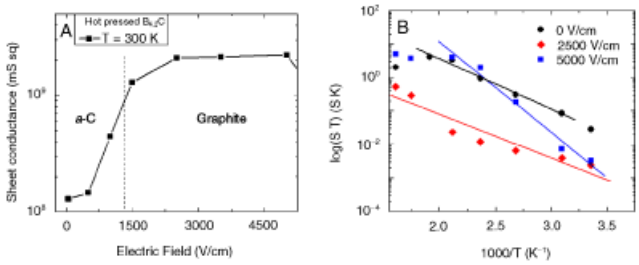

Fig. 2. (A) Sheet conductance of the boron carbide sample as a function of the applied electric field at room temperature. At low fields (below 3000 V/cm), the increase in conductance is attributed to the formation of an amorphous a-C(:B) phase, while at higher fields significant sp^2 clustering leads to a substantial increase of the aromatic cluster size. (B) Arrhenius plot of sheet conductance as a function of temperature at three different electric fields.

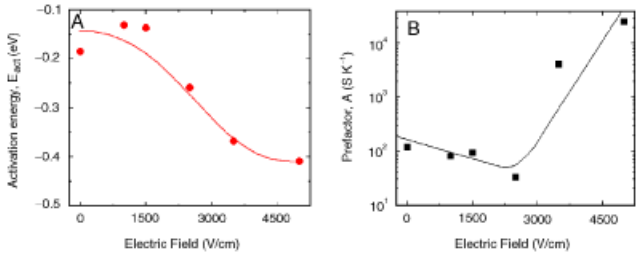

Fig. 3. Plot of (A) activation energy and (B) prefactor as a function of the electric field strength.

Long Branch, NJ) stabilized power supply. A programmable HP 4140B Picoammeter/Voltage (Agilent, Santa Clara, CA) source was used to measure its sheet conductance. The sample was heated in air by means of a Bayzi Thermopad microheater (Bayzi Corp., Cincinnati, OH). A thermocouple on the sample surface was used to record the temperature.

The room temperature sheet conductance measured *in situ* while recording the Raman spectra is shown in Fig. 2(A). The increase in conductance is an indicator of sp^2 clustering in B_4C, as confirmed by electrical measurements at higher temperatures. Typical electrical data as a function of temperature of the B_4C samples are shown in Fig. 2(B). The temperature behavior of electrical conductivity in B_4C at $T = 300$–600 K has been explained by Emin and colleagues[18,19] in terms of bipolaronic hopping between charged icosahedra (i.e., tunneling of both positive and negative charges through the icosahedra, activated by lattice vibrations). The expression of the conductance is therefore[18,19]:

$$S = A/T \cdot \exp(-E_{act}/k_B T) \tag{1}$$

where the prefactor A in high-purity $B_{4+x}C_{1-x}$ is found to depend on the carbon content, $1-x$. Emin and colleagues found that A decreases by approximately one order of magnitude when going from B_4C to B_9C.[18] Furthermore, because the theory indicates that the prefactor is related to the average distance r between charged icosahedra ($A \sim r^{-1}$),[18] any decrease of A reflects a lower icosahedron–icosahedron distance. At increasing boron content, this occurs because the chains connecting the icosahedra are progressively suppressed and the structure approaches that of boron, where icosahedra are closer.

In our case, the activation energy E_{act} depends on the size β of the potential well occupied by the polaron[18] according to

$$E_{act} \sim \beta^{-6}$$

In the absence of lattice degradation, β can be envisaged as the diameter of the icosahedra. In such a case, E_{act} is independent of the composition ranging from B_4C to B_9C. Rather, it has been suggested that the activation energy for electronic conduction is more closely related to the presence of impurities and imperfections, which act as further hopping sites.[18]

The prefactor and activation energy values (A and E_{act}) obtained in our work are plotted in Figs. 3(A) and (B). It can be observed that, for pulses below 3000 V/cm (corresponding to the regime of small or moderate segregation of amorphous carbon as detected by Raman), the prefactor decreases only slightly. This can be due to amorphization, which could be responsible for the observed changes in the Raman spectra. Within this regime, we find that the activation energy remains constant at approximately $E_{act} \approx -0.15 \pm 0.03$ eV. This value is very similar to that found by Emin and colleagues,[18,19] irrespective of the stoichiometry of the $B_{4+x}C_{1-x}$ samples hot pressed in vacuum (10^{-5}–10^{-6} Torr) at 2400 K from high-purity boron and carbon powders (B impurities below 30 ppm and C impurities below 10 ppm). This suggests that at electric fields below 3000 V/cm, the electrical transport mainly occurs through the boron carbide phase even though the Raman spectrum indicates the presence of free carbon.

For electric fields above 3000 V/cm, corresponding to significant formation and/or segregation of amorphous carbon clusters, the prefactor A increases with electric field strength. The activation energy trend is similar. The maximum E_{act} was measured to be -0.41 eV, an unexpectedly high value for boron carbide,[18,19] but consistent with hopping processes between nearest-neighbor sp^2 cluster islands in amorphous carbon.[20] In amorphous carbon, the conductivity can be described by Eq. (1), albeit the physical meaning of the activation energy and the prefactor are different.[20] E_{act} now represents the energy difference, with respect to the Fermi level of the defective electronic levels related to the presence of sevenfold or fivefold rings in the sp^2 cluster domains, while the prefactor assumes the form

$$A' \sim r'^2 \exp(-2r'/L) \tag{2}$$

where L is the sp^2 domain size and r' is the hopping distance between nearest-neighbor sp^2 cluster domains. Hence, a strong increase of the prefactor occurs when sp^2 clusters are generated and/or they increase in size and tend to coalesce.

This is exactly what we have observed in our *in situ* structural analysis with Raman spectroscopy. The charge transport mechanism obtained from conductivity versus temperature measurements is consistent with the fact that the application of voltage pulses of increasing electric field leads to the collapse of the B_4C structure. The transformation appears to occur sharply above a critical field of 3000 V/cm. Below this electric field value, Raman spectroscopy indicates the formation of amorphous phase but the prefactor (A) and the activation energy of charge transport show that the B_4C structure is essentially preserved. This suggests that the enhancement in conductivity and the D/G ratio may be due to intragranular segregation of carbon. Above 3000 V/cm, substantial segregation of amorphous carbon via an increase of the D/G ratio and the conductance can be inferred. Furthermore, at the maximum applied electric field of 5000 V/cm, the relatively large size of the segregated sp^2 clusters can be inferred from Raman spectroscopy. In addition to the Raman data, the continuous increase in the activation energy and a sharp rise in the prefactor above 3000 V/cm indicate a dramatic change in the transport properties. The high prefactor and activation energy measured at the maximum applied field are consistent with the formation of the large number and bigger sp^2 clusters and increased hopping between them, respectively. Thus, the structural changes obtained by Raman and transport data (prefactor and activation energy) are consistent with the local amorphization of B_4C with the application of electric fields. Because the presence of free carbon in our pristine samples was low, we believe that electric-field-induced amorphization is an intrinsic effect of B_4C. However, we cannot rule out the possibility that pristine intragranular carbon (which is a general feature of virtually all armor-grade B_4C samples[15]) lo-

cally acts as a "seed" for aggregation and clustering for the electric-field-induced sp^2 amorphous phase.

IV. Conclusions

In summary, we observed that electrical field pulses in boron carbide produce effects that appear to be similar to those induced by mechanical stress or shock impact. Specifically, amorphization and eventually large amorphous carbon clusters were detected using Raman spectroscopy during the application of pulses. The Raman features we measured as a function of the electric field could be similar to those obtained under shock or nanoindentation, although more detailed work is needed for confirmation. We have correlated our *in situ* Raman analysis with charge transport measurements, which are consistent with disruption of the boron carbide structure and production of sp^2 amorphous carbon clusters.

Acknowledgments

We would like to acknowledge Dr. R. C. McCuiston, Dr. J. La Salvia, and Dr. J. W. McCauley (US Army Research Laboratory, Aberdeen, MD) for supplying us with the boron carbide samples and for fruitful discussions.

References

[1]F. Thevenot, "Boron Carbide—A Comprehensive Review," *J. Eur. Ceram. Soc.*, **6**, 205–25 (1990).

[2]D. S. Cronin, G. McIntosh, C. Kaufman, K. Bul, and T. Berstad. 4th European LS-DYNA Users Conference Proceedings, DI47-57. Ulm, Germany, 2003.

[3]N. K. Bourne, "Shock-Induced Brittle Failure of Boron Carbide," *Proc. R. Soc. Lond. Ser. A-Math. Phys. Eng. Sci.*, **458**, 1999–2006 (2002).

[4]D. E. Grady, "Dynamic Properties of Ceramic Materials, SAND 94-32266," Sandia National Laboratory, 1995.

[5]M. W. Chen, J. W. McCauley, and K. J. Hemker, "Shock-Induced Localized Amorphization in Boron Carbide," *Science*, **299**, 1563–6 (2003).

[6]G. Fanchini, J. W. McCauley, and M. Chhowalla, "Behavior of Disordered Boron Carbide Under Stress," *Phys. Rev. Lett.*, **97**, 035502 (2006).

[7]V. Domnich, Y. Gogotsi, M. Trenary, and T. Tanaka, "Nanoindentation and Raman Spectroscopy Studies of Boron Carbide Single Crystals," *Appl. Phys. Lett.*, **81** [20] 3783–5 (2002).

[8]D. Ge, V. Domnich, T. Juliano, E. A. Stach, and Y. Gogotsi, "Structural Damage in Boron Carbide Under Contact Loading," *Acta Mater.*, **52**, 3921 (2002).

[9]D. Ghosh, G. Subhash, C. H. Lee, and Y. K. Yap, "Strain-Induced Formation of Carbon and Boron Clusters in Boron Carbide During Dynamic Indentation," *Appl. Phys. Lett.*, **91**, 61910 (2007).

[10]X. Q. Yan, W. J. Li, T. Goto, and M. W. Chen, "Raman Spectroscopy of Pressure-Induced Amorphous Boron Carbide," *Appl. Phys. Lett.*, **88** [131905] 3 (2006).

[11]J. La Salvia, R. C. McCuiston, G. Fanchini, J. W. McCauley, M. Chhowalla, H. T. Miller, and D. E. MacKenzie, "Shear Localization in Sphere-Impacted Armor-Grade Boron Carbide"; *Proceedings of the 23rd International Symposium on Ballistics, Tarragona, Spain, TB49, 2007*.

[12]G. Fanchini, V. Gupta, A. B. Mann, and M. Chhowalla. submitted (2007).

[13]R. R. Lazzari, N. Vast, J. M. Besson, S. Baroni, and A. Dal Corso, "Atomic Structure and Vibrational Properties of Icosahedral B_4C Boron Carbide," *Phys. Rev. Lett.*, **83** [16] 3230–3 (1999).

[14]K. Shirai and S. Emura, "Lattice Vibrations and the Bonding Nature of Boron Carbide," *J. Phys.:Condens. Matter*, **8** [50] 10919–29 (1996).

[15]M. W. Chen, J. W. McCauley, J. C. LaSalvla, and K. J. Hemker, "Microstructural Characterization of Commercial Hot-Pressed Boron Carbide Ceramics," *J. Am. Ceram. Soc.*, **88** [7] 1935–42 (2005).

[16]A. C. Ferrari and J. Robertson, "Resonant Raman Spectroscopy of Disordered, Amorphous, and Diamond-Like Carbon," *Phys. Rev. B*, **64** [7] 075414 (2001).

[17]G. Fanchini, A. Tagliaferro, and S. C. Ray, "Electronic and Vibrational Structures of Amorphous Carbon Nitrides," *Diam. Rel. Mater.*, **12**, 208 (2003).

[18]G. A. Samara, D. Emin, and C. Wood, "Pressure and Temperature Dependences of the Electronic Conductivity of Boron Carbides," *Phys. Rev. B*, **32** [4] 2315–8 (1985).

[19]C. Wood and D. Emin, "Conduction Mechanism in Boron Carbide," *Phys. Rev. B*, **29** [8] 4582–7 (1984).

[20]D. Dasgupta, F. Demichelis, and A. B. Tagliaferro, "Electrical Conductivity of Amorphous Carbon and Amorphous Hydrogenated Carbon," *Phil. Mag. B*, **63** [6] 1255–66 (1991). □